Insulator-metal like transition in air-synthesized Mn^{4+}-rich $La_{1-x}Ba_xMnO_3$: grain boundary phase effect

2002 J. Phys.: Condens. Matter 14 1297

(http://iopscience.iop.org/0953-8984/14/6/316)

INSTITUTE OF PHYSICS PUBLISHING JOURNAL OF PHYSICS: CONDENSED MATTER

J. Phys.: Condens. Matter **14** (2002) 1297–1306 PII: S0953-8984(02)31380-8

Insulator–metal like transition in air-synthesized Mn^{4+}-rich $La_{1-x}Ba_xMnO_3$: grain boundary phase effect

B Raveau[1], **C Martin, A Maignan and M Hervieu**

Laboratoire CRISMAT, UMR 6508 associée au CNRS, ISMRA et Université de Caen 6 Boulevard du Maréchal Juin, 14050 CAEN Cedex 4, France

E-mail: bernard.raveau@ismra.fr

Received 29 November 2001
Published 1 February 2002
Online at stacks.iop.org/JPhysCM/14/1297

Abstract

The air-synthesized $La_{1-x}Ba_xMnO_3$ system was revisited for $0.4 \leqslant x \leqslant 0.9$. We show that this system exhibits an insulator–metal like transition, T_{IM} (175–230 K), far below the Curie temperature ($T_C \approx 335$ K). In contrast to previous studies, we demonstrate that this system is multiphase, i.e. involving a hexagonal phase and a ferromagnetic cubic perovskite. We suggest that the T_{IM} transition at low temperature is due to the presence of a secondary perovskite at the grain boundary. In less oxidizing conditions, the synthesis of cubic perovskites for $x \approx 0.50$, with T_{IM} ranging from 170 to 240 K, supports this interpretation. Tunnelling magnetoresistance up to 22% at 10 K under 0.2 T is also observed.

1. Introduction

Among the various manganese perovskites with colossal magnetoresistance (CMR) properties, the $La_{1-x}Ba_xMnO_3$ manganites are of great interest because of their high Curie temperature which can reach values up to 360 K. The main compounds that were studied, in a first step, for this series, corresponded to the hole doped region around $x \approx 1/3$ [1–6]. This composition range is thought to be optimal for developing the strongest double exchange (DE) interactions between Mn^{3+} and Mn^{4+} cations [7] which favour the transition to a ferromagnetic metallic (FMM) state.

The crystal chemistry of these oxides is in fact complex [6], due to the eventual formation of hexagonal $BaMnO_3$-type perovskites when the synthesis is carried out in air, so that the physics of the Mn^{4+}-rich barium manganites has not been investigated in detail to date. Nevertheless the homogeneity range of these oxides could be extended up to $x = 0.50$ using a two-step synthesis mode [8, 9]. The latter studies show that order–disorder phenomena between La^{3+} and Ba^{2+} cations may dramatically affect the Curie temperature of $La_{0.5}Ba_{0.5}MnO_3$, with T_C

[1] Author to whom any correspondence should be addressed.

ranging from 270 K for the disordered phase to 335 K for the ordered oxide. Moreover the study of $La_{1-x}Ba_xMnO_3$ polycrystalline ceramics is made difficult by the possible existence of grain boundary effects, observed in the form of a shoulder at 254 K on the $\rho(T)$ curve of $La_{0.67}Ba_{0.33}MnO_3$, besides the peak at $T_C = 330$ K, by Ju and Sohn [10].

In a recent study, Yuan *et al* [11] claim to have discovered a new perovskite in the highly Mn^{4+}-doped region ($x \approx 2/3$), $La_{1/3}Ba_{2/3}MnO_3$, with an orthorhombic symmetry which exhibits an insulator–metal (IM) transition at $T_{IM} \approx 230$ K. According to these authors, the magnetoresistance observed for this phase under low magnetic field and its ferromagnetic ordering are unlikely to be due to the DE mechanism, but originate from superexchange-type interactions. Bearing in mind these new results, we have revisited the Mn^{4+}-rich $La_{1-x}Ba_xMnO_3$ system synthesized in air ($x \geqslant 0.4$), with particular attention to the $x = 2/3$ composition. We show that this system exhibits a broad maximum in resistivity at low temperature over a large composition range $x \approx 0.4$–0.75. The latter is similar to the insulator–metal like transitions observed by different authors in manganites, but with a transition temperature T_{IM} ranging from 175 to 230 K, far below the Curie temperature which remains approximately constant in the whole domain, $T_C = 335$ K. In contrast to previous authors [11], we demonstrate that the system is multiphase, involving two main phases, with a hexagonal and a cubic symmetry, the second one with $x \approx 0.35$ being ferromagnetic. We interpret the T_{IM} transition at low temperature by the formation of a secondary perovskite at the grain boundaries. This grain boundary effect is in agreement with the results obtained by Ju and Sohn [10] for $La_{0.67}Ba_{0.33}MnO_3$, and moreover is supported by the synthesis of the pure cubic perovskites in less oxidizing conditions, for $x \approx 0.50$, with $170\ \text{K} \leqslant T_{IM} \leqslant 240\ \text{K}$.

2. Experiment

The air-synthesized ceramic samples with nominal compositions $La_{1-x}Ba_xMnO_3$ were prepared by mixing La_2O_3, $BaCO_3$ and Mn_2O_3 in stoichiometric proportions. The mixtures were first heated at 1000 °C for 12 h to achieve decarbonation. The resulting powders were then pressed in the form of pellets under 1 tonne cm^{-2} pressure and sintered at 1200 °C for 12 h and 1500 °C for 12 h in air. The products were then cooled down to 800 °C at 5 °C h^{-1} and finally quenched to room temperature.

The Ar-synthesized ceramic samples were fabricated using an identical method except that air was replaced by an argon flow containing a few per cent O_2. In that case the samples were cooled under the Ar flow at 5 °C h^{-1} down to room temperature.

The x-ray powder diffraction (XRPD) patterns were registered at room temperature with a Philips diffractometer, using Cu K_α radiation. The electron diffraction and electron microscopy study was performed with JEOL 200CX and TOPCON 002B microscopes, both equipped with a Kevex analyser for energy dispersive spectroscopy (EDS). Oxygen stoichiometry was deduced from chemical titration. Magnetization measurements were carried out after zero-field cooling from 5 to 400 K using a SQUID magnetometer and a vibrating sample magnetometer.

Resistivity was measured between 5 and 400 K on bars with dimensions $0.2 \times 0.2 \times 1\ cm^3$, using a standard four-point method. Magnetoresistance measurements were performed in a magnetic field up to 7 T with temperatures ranging from 5 to 300 K.

3. Results

3.1. Air-synthesized $La_{1-x}Ba_xMnO_3$: mixtures of hexagonal and cubic perovskites

The evolution of the XRPD patterns versus composition shows that, whatever the value of x in the range from 0.4 to 0.9, they contain two sets of peaks characteristic of the

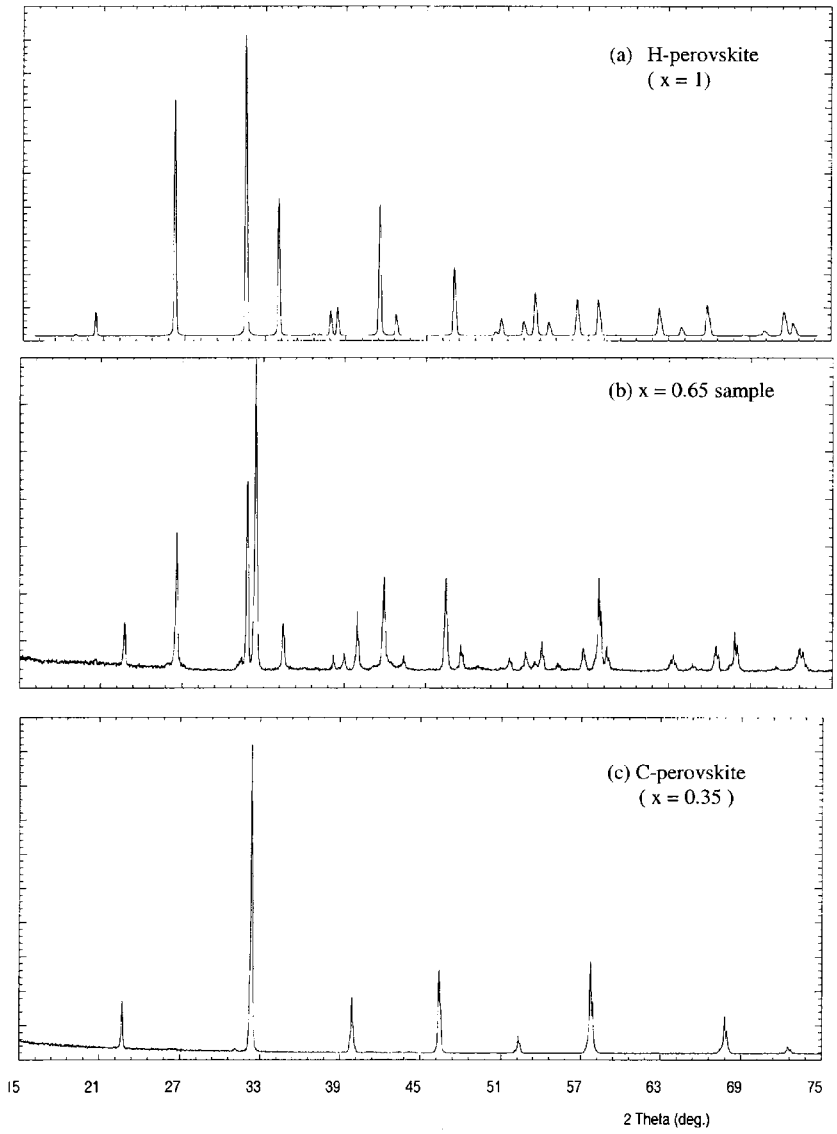

Figure 1. XRPD patterns of (*a*) hexagonal (H) $BaMnO_{3-x}$ from [15], (*b*) air-synthesized $La_{0.35}Ba_{0.65}MnO_3$ and (*c*) cubic (C) perovskite $La_{0.65}Ba_{0.35}MnO_3$.

hexagonal and cubic perovskites. This is illustrated by comparing the XRPD patterns of the composition $La_{0.35}Ba_{0.65}MnO_3$ (figure 1(*b*)) with those of the hexagonal (H) perovskite $BaMnO_{3-\delta}$ (figure1(*a*)) and of the cubic (C) perovskite $La_{0.65}Ba_{0.35}MnO_3$ (figure 1(*c*)). The electron microscopy study of the $La_{0.35}Ba_{0.65}MnO_3$ sample and the coupled energy dispersive analysis (EDS) carried out on more than 50 microcrystals confirm that this sample consists of two main phases. One set of crystals, which are found to have the cationic composition '$La_{0.1}Ba_{0.9}Mn$', exhibit (110) ED patterns (figure 2) characteristic of the hexagonal perovskite. Most of the crystallites exhibit a $4L$ structure, ($a \sim 5.67$ Å, $b \sim 9.3$ Å), as shown in figure 2(*a*), and the others consist of irregular hexagonal polytypes as observed from the

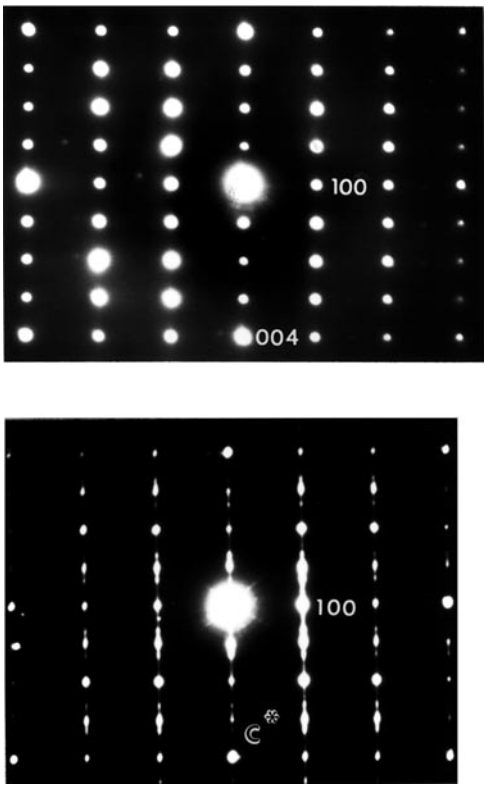

Figure 2. [110] ED patterns of the hexagonal perovskite-type microcrystals with '$La_{0.1}Ba_{0.9}Mn$' cationic composition observed in the sample synthesized in air with the nominal composition $La_{0.35}Ba_{0.65}MnO_3$: (*a*) regular $4L$ structure, (*b*) disordered polytypes.

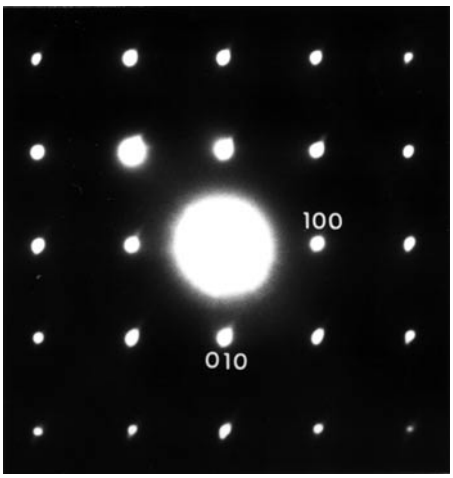

Figure 3. [001] ED pattern of the cubic perovskite type microcrystals with '$La_{0.65}Ba_{0.35}Mn$' cationic composition observed in the same sample as figure 2, that is air synthesized and $La_{0.35}Ba_{0.65}MnO_3$ as nominal composition.

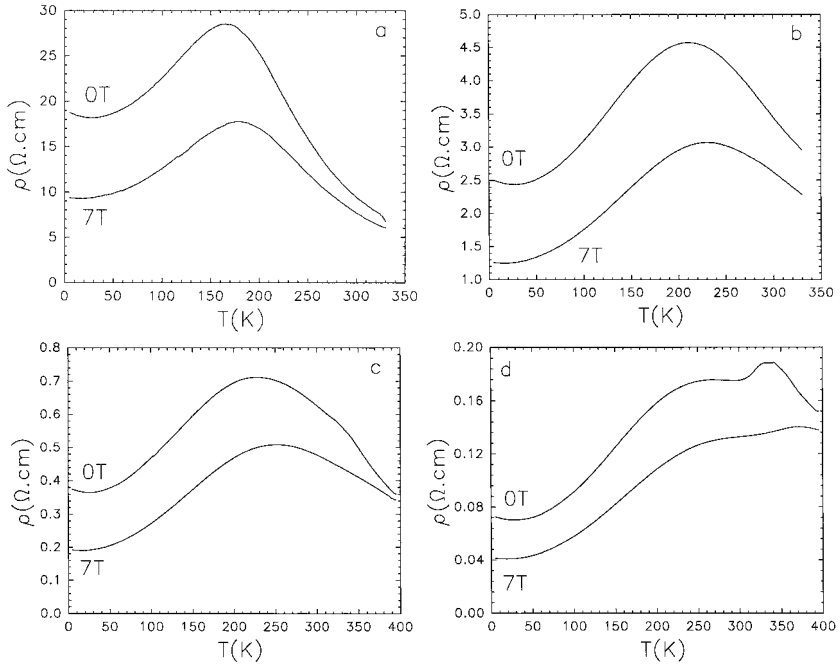

Figure 4. $\rho(T)$ curves of air-synthesized $La_{1-x}Ba_xMnO_3$: (*a*) $x = 0.74$ (29% of $La_{0.65}Ba_{0.35}MnO_3$), (*b*) $x = 0.65$ (45.5% of $La_{0.65}Ba_{0.35}MnO_3$), (*c*) $x = 0.52$ (69.1% of $La_{0.65}Ba_{0.35}MnO_3$), (*d*) $x = 0.49$ (74.5% of $La_{0.65}Ba_{0.35}MnO_3$).

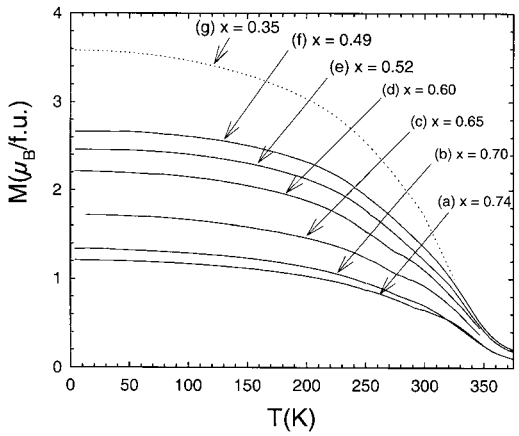

Figure 5. Magnetization curves $M(T)$ of air-synthesized $La_{1-x}Ba_xMnO_3$: (*a*) $x = 0.74$, (*b*) $x = 0.70$, (*c*) $x = 0.65$, (*d*) $x = 0.60$, (*e*) $x = 0.52$, (*f*) $x = 0.49$, (*g*) $x = 0.35$.

streaks along c^* in figure 2(*b*). The second set of crystals, with the cationic composition '$La_{0.65}Ba_{0.35}Mn$', exhibit [001] ED patterns (figure 3) characteristic of the classical cubic perovskite ($a \approx 3.91$ Å) previously identified by different authors [1–6, 8–10]. Thus this $La_{0.35}Ba_{0.65}MnO_3$ sample, as well as the sample prepared by Yuan *et al* [11] which exhibits an identical XRD pattern, have at least two phases and this multiphase character exists in the whole range of compositions $0.4 < x < 0.9$.

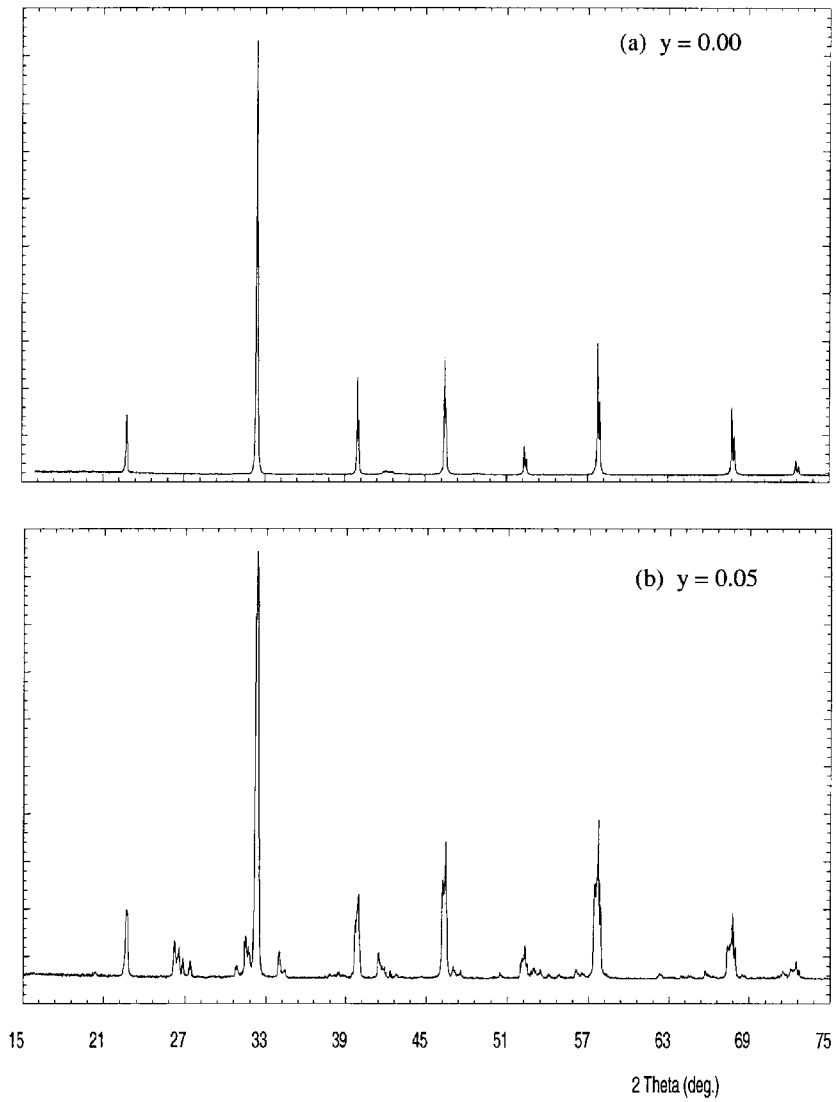

Figure 6. XRPD patterns of argon-synthesized $La_{0.5}Ba_{0.5}MnO_3$ (*a*) and $La_{0.45}Ba_{0.55}MnO_3$ (*b*).

3.2. The insulator–metal-like transition in multiphase $La_{1-x}Ba_xMnO_3$

In spite of their two-phase character, these $La_{1-x}Ba_xMnO_3$ samples are of great interest due to the existence of an IM transition first pointed out by Yuan *et al* [11] for $x = 2/3$. The systematic investigation of the $\rho(T)$ curves for different air-synthesized compositions (figure 4) shows an IM transition characterized by a peak, whatever the value of x in the range 0.5 to 0.75, whereas for $x > 0.75$ the samples are insulators. Below $x = 0.50$, the $\rho(T)$ curves show either a second peak or a shoulder around 330 K besides a plateau which starts at 230 K (see for instance the curve $x = 0.49$ in figure 4(*d*)). More importantly, we observe that the transition temperature T_{IM} varies with the composition, increasing significantly as x decreases, from T_{IM} = 175 K for $x = 0.74$ to 230 K for $x = 0.52$. Concomitantly, the room-temperature

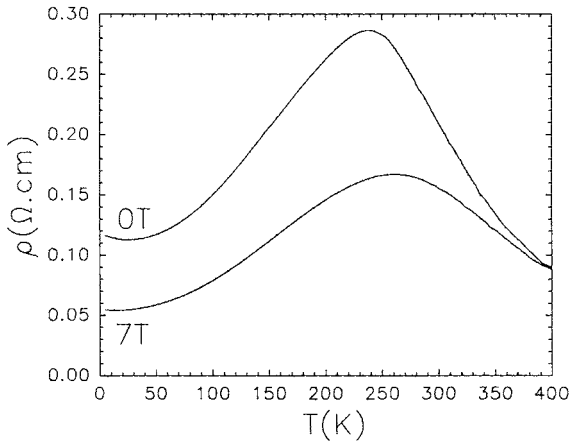

Figure 7. Resistivity curves $\rho(T)$ of argon-synthesized $La_{0.5}Ba_{0.5}MnO_3$.

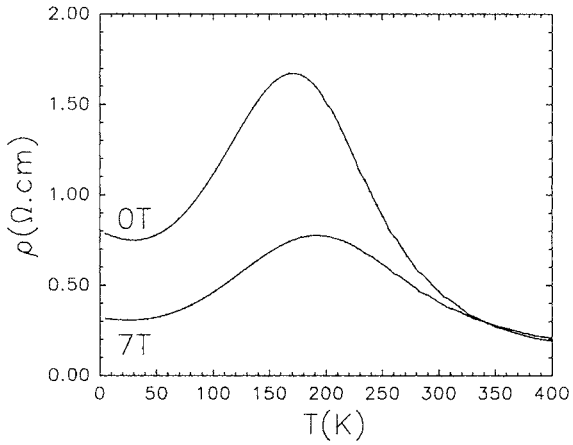

Figure 8. Resistivity curves $\rho(T)$ of argon-synthesized $La_{0.47}Ba_{0.53}MnO_3$.

resistivity of the samples decreases with x, ranging from 9 Ω cm for $x = 0.74$ to 0.6 Ω cm for $x = 0.52$ (figures 4(a) and (c)). It is worth pointing out that the transition temperature T_{IM}, although quite reproducible, may vary by about 20 K for the same nominal composition, by changing the experimental conditions (sintering temperature, speed of cooling etc). This suggests that the IM transition is not an intrinsic property of the bulk but depends on the nature of the ceramic (microstructure, homogeneity...). This viewpoint is supported by the magnetic properties of these air-synthesized samples. The corresponding $M(T)$ curves (figure 5) show that the samples are ferromagnetic with a unique Curie temperature, $T_C \approx 335$ K, whatever the value of x, much higher than the T_{IM} values. Thus, T_{IM} is not connected to the bulk ferromagnetism observed in those ceramic samples. In contrast, the values of the magnetic moment at 5 K, ranging from $M = 1.2\ \mu_B$ for $x = 0.74$ to $M = 3.6\ \mu_B$ for $x = 0.35$, are in perfect agreement with the results of the coupled ED/EDS study. The latter inded shows that the different samples correspond to a mixture of two types of crystals corresponding to the hexagonal perovskite $Ba_{0.9}La_{0.1}MnO_{3-\delta}$ and to the cubic perovskite $La_{0.65}Ba_{0.35}MnO_3$. Taking into consideration the results obtained by different authors [1–6, 8–10] the second

Table 1. Observed and calculated magnetic moments at 5 K for the air-synthesized mixtures $La_{1-x}Ba_xMnO_3$ of H($La_{0.1}Ba_{0.9}MnO_3$) and C($La_{0.65}Ba_{0.35}MnO_3$) manganites ($M_{5\ K} = 3.6\mu_B$ for FM $La_{0.65}Ba_{0.35}MnO_3$).

x	$M_{observed}$ (μ_B)	$M_{calculated}$ (μ_B)	$La_{0.65}Ba_{0.35}MnO_3$%
0.74	1.20	1.05	29.0
0.70	1.34	1.30	36.4
0.65	1.70	1.63	45.5
0.60	2.20	1.96	54.5
0.52	2.45	2.49	69.1
0.49	2.65	2.68	74.5

phase alone should be responsible for ferromagnetism and metallicity in this system. The calculated magnetic moments deduced from these observations are in rather good agreement with the experimental values (table 1) for different values of x, showing that the two main phases which form these ceramics are the hexagonal perovskite $La_{0.1}Ba_{0.9}MnO_3$, which is an insulating antiferromagnet, and the cubic perovskite $La_{0.65}Ba_{0.35}MnO_3$, which is FMM below 335 K. For $x \leqslant 0.74$, the mixture contains more than 29% of the FMM phase, so that the percolation threshold is exceeded and the ceramics should exhibit a metallic conductivity, whatever the value of x, for $T < 335$ K as for the pure cubic hole doped FMM perovskite $La_{0.65}Ba_{0.35}MnO_3$, in agreement with the DE mechanism previously invoked for this oxide. On the other hand, the superexchange mechanism, based on the bending of Mn–O–Mn bonds away from 180° [12], cannot be applied here to explain the semiconductor to metal transition far below T_C, at least as an intrinsic mechanism in the grains, since the only phase which is not cubic is the hexagonal one which does not exhibit any IM transition. A rather similar $\rho(T)$ behaviour was observed for $La_{0.67}Ba_{0.33}MnO_3$ [10] which shows an additional shoulder at 254 K besides the peak at $T_C = 330$ K, and for $Nd_{0.7}Ba_{0.3}MnO_3$ [13] which displays a second bump at 90 K below the peak at $T_C = 140$ K, in spite of the monophasic character of those samples. Such a property was explained by Ju and Sohn [10] on the basis of grain boundary effects. Based on these considerations, we can propose that a filamentary FMM perovskite, with a lower $T_C = T_{IM}$, is formed at the grain boundaries of these ceramics during sintering in air. This filamentary perovskite should have a composition different from that of the $La_{0.65}Ba_{0.35}MnO_3$ cubic perovskite observed in the mixtures of the air-sintered ceramics. This phase is present in amounts which are too small to be detected by XRPD and ED techniques. The possibility of synthesizing a cubic perovskite, $La_{0.5}Ba_{0.5}MnO_3$, with a T_C around 270 K by a two-step method [8,9], first heating the oxides in argon and then annealing them in oxygen at a lower temperature, supports this viewpoint. Nevertheless, such a scenario implies the possible existence of FMM perovskites with T_C ranging from 175 to 230 K. In order to check this point, attempts have been made to synthesize pure perovskites close to the composition $La_{0.5}Ba_{0.5}MnO_3$ using the same protocol as that for the air-synthesized ceramics, but replacing air by an argon flow.

3.3. The argon-synthesized $La_{0.5-y}Ba_{0.5+y}MnO_{3-\delta}$ perovskites

For the experimental conditions described above a pure cubic perovskite $La_{0.5}Ba_{0.5}MnO_{3-\delta}$ is obtained, as shown from the XRPD pattern (figure 6(*a*)). But the purity of the sample is very sensitive to the cationic composition, since for $La_{0.45}Ba_{0.55}MnO_{3-\delta}$ a mixture of two cubic perovskites, in the presence of small amounts of the hexagonal perovskite, is obtained (figure 6(*b*)). The EDS analysis of numerous microcrystals of the pure $La_{0.5-y}Ba_{0.5+y}MnO_{3-\delta}$

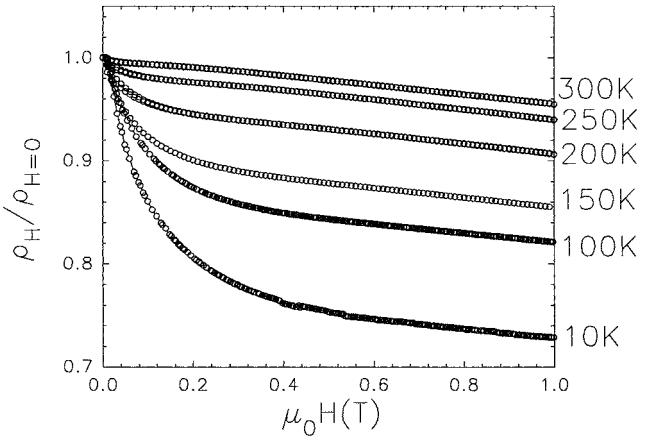

Figure 9. $\rho(H)$ curves at various temperatures for air-synthesized $La_{0.40}Ba_{0.60}MnO_3$ ceramic.

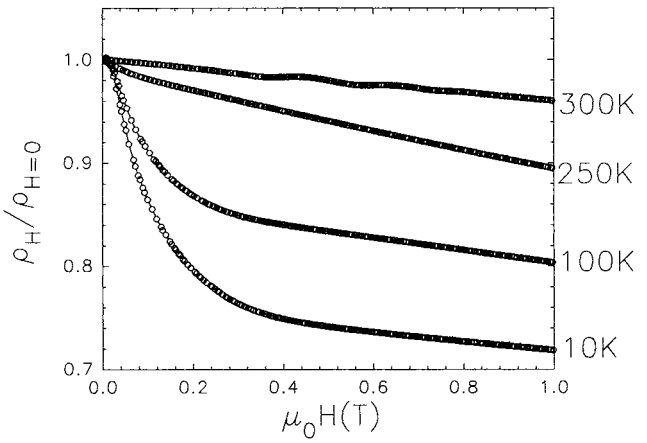

Figure 10. $\rho(H)$ curves at various temperatures for the pure $La_{0.5}Ba_{0.5}MnO_3$ synthesized under an argon flow.

perovskites, corresponding to $y = 0.00$ and 0.03, confirms the high homogeneity of the samples and their nominal cationic compositions, whereas the chemical analysis leads to the formulation $La_{0.5-y}Ba_{0.5+y}MnO_3$. The $La_{0.5}Ba_{0.5}MnO_3$ and $La_{0.47}Ba_{0.53}MnO_3$ $\rho(T)$ curves (figures 7, 8) show that these oxides exhibit semiconductor to metal transitions at $T_{IM} \approx 240$ and 170 K respectively. These results are of great interest, since they demonstrate that, in this compositional region ($x \approx 0.50$), the T_{IM} values are very sensitive to the cationic composition. Let us recall that the stability of these perovskites also depends on the oxygen stoichiometry and on the thermal treatment (order–disorder phenomena in the cationic sublattice) used for the synthesis. The presence of the $La_{0.5}Ba_{0.5}MnO_3$ type perovskite as a filamentary phase at the grain boundaries can explain perfectly the insulator–metal transition temperatures ($T_{IM} \approx 175$ to 230 K), lower than that of the main phase $La_{0.65}Ba_{0.35}MnO_3$ ($T_{IM} \approx T_C \approx 335$ K), since it hinders the conduction path between the grains above a certain temperature.

3.4. Low-field magnetoresistance

The $\rho(T)$ curves of the $La_{1-x}Ba_xMnO_3$ air-synthesized samples registered under a magnetic field of 7 T (figure 4) clearly show a large negative magnetoresistance. The $La_{0.4}Ba_{0.6}MnO_3$ $\rho(T)$ curves (figure 9) registered at various temperatures show that the resistance falls abruptly in fields smaller than 0.2 T and more slowly in higher fields, in agreement with the results previously observed for $La_{1/3}Ba_{2/3}MnO_3$ [10]. This abrupt increase of magnetoresistance in low fields increases significantly as the temperature decreases, $\Delta\rho/\rho$ reaching 22% under 0.2 T at 10 K whatever the value of x from 0.40 to 0.75. This type of evolution, already observed for $La_{2/3}Ba_{1/3}MnO_3$ thin films, is characteristic of tunnelling magnetoresistance (TMR), which appears at the grain boundary.

Similar $\rho(H)$ curves registered for the Ar-synthesized $La_{0.5}Ba_{0.5}MnO_3$ sample (figure 10) show that the magnetoresistance, at low and high magnetic fields, is similar to that of the $La_{0.4}Ba_{0.6}MnO_3$ multiphase sample prepared in air. The similarities of the magnetoresistance for the pure cubic phase and the multiphase one shows that the hexagonal phase does not play a role in the observation of the low-field magnetoresistance.

3.5. Conclusion

In this study we have shown that the air-synthesized $La_{1-x}Ba_xMnO_3$ ceramics contain at least two phases, consisting of a mixture of hexagonal and cubic perovskites, and that a new FMM perovskite, $La_{0.5-y}Ba_{0.5+y}MnO_3$, with $T_{IM} \approx 170$–240 K can be synthesized. The presence of the latter as a filamentary phase at the grain boundaries of the air-synthesized $La_{1-x}Ba_xMnO_3$ ceramics is suggested to explain the insulator–metal transitions, with T_{IM} ranging from 175 to 230 K in those materials. These results demonstrate that the DE mechanism remains valid in these oxides, as well as in the air-synthesized ceramics such as the pure $La_{0.5}Ba_{0.5}MnO_3$ perovskite ceramics, in contrast to what was claimed by Yuan *et al* [11].

References

[1] von Helmolt R, Wecker J, Holzapfel B, Schultz L and Samner K 1993 *Phys. Rev. Lett.* **71** 2331
[2] Xiong G C, Li Q, Ju L H, Greene R L and Venkatesan T 1995 *Appl. Phys. Lett.* **66** 1689
[3] Jirak Z, Pollert E, Andersen A F, Grenier J C and Hagenmuller P 1990 *Eur. J. Solid State Inorg. Chem.* **27** 421
[4] Radaelli P G, Marezio M, Hwang H Y and Cheong S W 1996 *J. Solid State Chem.* **122** 444
[5] Ju H L, Gopalakrishnan J, Peng J L, Xiong G C, Venkatesan T and Greene R L 1994 *Phys. Rev.* B **51** 6143
[6] Dabrowski B, Rogacki K, Xiong X, Klamut P W, Dybzinski R, Shaffer J and Jorgensen J D 1998 *Phys. Rev.* B **58** 2716
[7] Zener C 1951 *Phys. Rev.* **82** 403
[8] Barnabé A, Millange F, Maignan A, Hervieu M and Raveau B 1998 *Chem. Mater.* **10** 252
[9] Millange F, Caignaert V, Domengès B and Raveau B 1998 *Chem. Mater.* **10** 1974
[10] Ju H L and Sohn H 1997 *Solid State Commun.* **102** 463
[11] Yuan S L, Jiang Y, Zeng X Y, Zhao W Y, Yang Y P, Qian J P, Zhang G Q, Tu F and Tang C Q 2000 *Phys. Rev.* B **62** 11 347
[12] Goodenough J B 1976 *Magnetism and the Chemical Bond* (New York: Krieger) p 184
[13] Maignan A, Martin C, Hervieu M, Raveau B and Hejtmanek J 1998 *Solid State Commun.* **107** 363
[14] Shreekala R, *et al* 1997 *Appl. Phys. Lett.* **71** 282
[15] Hardy A 1962 *Acta Crystallogr.* **15** 179